Simultaneous Segmentation of Multiple Retinal Pathologies Using Fully Convolutional Deep Neural Network

Maryam Badar, M. Shahzad, M.M. Fraz
School of Electrical Engineering and Computer Science
National University of Sciences and Technology, Islamabad, Pakistan
mbadar.mscs16seecs.seecs.edu.pk, muhammad.shehzad@seecs.edu.pk,
moazam.fraz@seecs.edu.pk

Abstract. The segmentation of retinal pathologies is the primitive and essential step in the development of automated diagnostic system for various systemic, cardiovascular, and ophthalmic diseases. The existing state-of-the-art machine learning based retinal pathologic segmentation techniques mainly aim at delineating pathology of one kind only. In this context, we have proposed a novel end-to-end technique for simultaneous segmentation of multiple retinal pathologies (i.e., exudates, hemorrhages, and cotton-wool spots) using encoder-decoder based fully convolutional neural network architecture. Moreover, the task of retinal pathology extraction has been modeled as a semantic segmentation framework which enables us to obtain pixel-level class labels. The proposed algorithm has been evaluated on publically available Messidor dataset and achieved state-of-the-art mean accuracies of 99.24% (exudates), 97.86% (hemorrhages), and 88.65% (cotton-wool spots). The developed approach may aid in further optimization of pathology quantification module of the QUARTZ software which has been developed earlier by our research group.

Keywords: Retinal Pathology, Diabetic Retinopathy, Deep Learning, Fully Convolutional Neural Networks, Encoder-Decoder, Semantic Segmentation

1 Introduction

Human retina is a non-invasive window to human circulatory system; therefore, automated analysis of human retina has potential to reveal important information about ocular as well as the systemic diseases such as Age-related Macular Degeneration (AMD) and Glaucoma, Diabetic Retinopathy (DR), Diabetic Macular edema, Hypertensive retinopathy and multiple sclerosis [1]. A clear in-vivo view of the retina and vascular flow could help in the process of important structural and functional information extraction from retina thereby assisting the clinicians in timely and accurate diagnosis. The advancements in image acquisition modalities during the last 160 years allow non-invasive imaging of retina thus leading to efficient retinal landmarks extraction, pathology detection and disease classification.

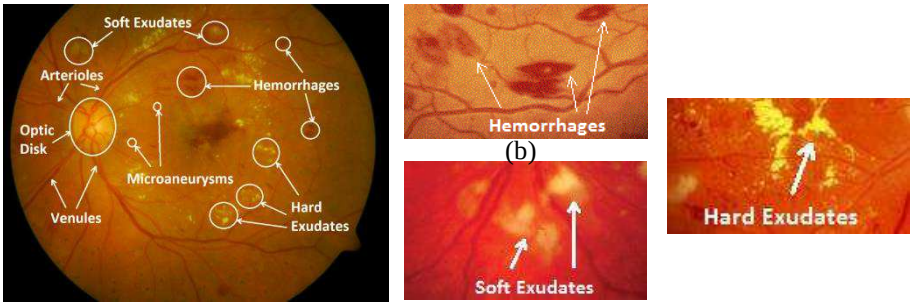

(a) (b) (c) (d)

Fig. 1. (a) Retinal image with pathologies (b) Hemorrhages (c) Soft Exudates (d) Hard Exudates

DR is a chronic progressive sight-threatening disease. It contributes to 4.8% of the 37 million cases of blindness throughout the world [2]. Due to the lack of resources, 50% of the patients miss their ophthalmic examination sessions leading to irreversible damage to visual acuity. Timely treatment of DR can reduce the threat to visual acuity by 60% [3] therefore diagnosis of DR at the premature stage is very important. Manual segmentation techniques adopted by clinicians are monotonous, time-consuming, inconvenient, labor intensive, observer driven, and require proficient skill [4] whereas computer-aided detection of retinal abnormalities is cost-effective, feasible, objective, and doesn't require efficiently trained clinicians to grade the images [1]. Moreover, the automated retinal image analysis has the ability to provide the timely diagnosis provisions. These techniques are not a replacement to the ophthalmologists rather the automated screening systems have the potential to assist the ophthalmologists in large-scale screening programs by allowing cost-effective and accurate diagnosis. Automatic classification of DR through analysis of retinal images has become an established practice in ophthalmology. But these gradings are not specific to the types of lesions present in retinal images therefore segmented retinal pathology (exudates, hemorrhages, and cotton wool spots) will assist the clinicians in grading.

The anatomy of retinal pathology varies with the types of lesions. Exudates appear as a consequence of leakage of fats and proteins along with water from abnormally permeable walls of retinal vessels. However, cotton wool spots surface in large retinal regions which become deprived of oxygen due to blockage in arterioles. They emanate as fluffy white patches in the ocular fundus [5]. The blockade in arterioles may instigate a pressure build up within the vessels. Significant amount of pressure could burst the vessels and result in origination of hemorrhages [5] as represented in **Fig. 1**. The segmentation of these pathologies is a challenging and intricate task because their color intensities lie in close proximity to that of other ocular structures.

Unprecedented achievements in classification tasks via Deep Learning techniques in contemporary years call for their application in retinal image analysis [6]. A few deep learning based techniques have been developed for classifying the presence/absence of certain kind of retinal pathological structures. These methods can

localize the presence of retinal pathology but cannot precisely extract the boundary of pathology through pixel-wise segmentation.

We propose an encoder-decoder based deep convolutional neural network architecture for simultaneously segmenting the retinal exudates, hemorrhages, and cotton wool spots. The network assigns each pixel to one of the four classes: hemorrhages, exudates, cotton-wool-spots, or background. The task of retinal pathology segmentation has been modeled as a semantic segmentation problem. This type of pixel-wise segmentation delineates each pixel as belonging to a particular object class. To the limit of our knowledge, this is the first attempt which provides a deep learning based end-to-end system for pixel wise segmentation of multiclass retinal pathologies simultaneously. This work can be further extended to build a computer aided DR grading system based on segmented retinal pathology which can assist the human graders as well as improving the health care globally.

In the rest of the paper we illustrate a review of the related literature in section 2, the detailed description of proposed methodology in section 3, and description of experiments and evaluation in section 4. The last section is dedicated to discussions and conclusion.

2 Related Work

A number of template, edge, and morphology based algorithms have been presented in the past for auto delineation of retinal landmarks [7] and retinal pathology [8, 9]. Several supervised and unsupervised neural networks based methods have also been employed for retinal image analysis. Many supervised methodologies adopted Multi-Layer Perceptron (MLP), Support Vector Machine (SVM), Artificial Neural Network (ANN) and decision trees [10, 11]. Similarly, matched filtering and model based approaches have been scrutinized for the purpose of unsupervised retinal abnormality detection [4, 12]. All of traditional methods required manual feature designing through Scale-invariant Feature Transform (SIFT), Speeded-Up Robust Features (SURF), , and Histogram of Oriented Gradients (HOG) feature descriptors [13, 14]. The explicit domain knowledge is mandatory for this kind of hand crafted feature extraction [6]. Most of the times, the results obtained through them are more specialized on a dataset and generalization is not achieved. Recent advancements in visual recognition via deep learning have invigorated researchers to employ these techniques in the field of ophthalmology as well. Automatic learning of intricate features in the retinal images can be obtained by the use of Deep Neural Networks (DNN). DNN is a form of ANN in which arrangement of neurons is inspired by neuron disposition of animal visual cortex. DNN provides the hierarchical feature extraction with limited preprocessing of input images hence does not use hand crafted features [6].

Exudates appear as a consequence of leakage of lipids and proteins along with water from abnormally permeable walls of retinal vessels. Segmentation of exudates holds an imperative position for diagnosis of DR. A hybrid method involving deep learning methods and traditional image processing methods has been adopted by Prentasic et al., [15] to segment exudates from retinal images. They used traditional

image processing methods to generate probability maps of retinal anatomical structures. These probability maps were then combined with the output probability map generated by their 10 layered Convolutional Neural Network (CNN) to decrease the number of false positives. The effectiveness of the DNN based method is directly dependent on the size of dataset therefore size of dataset is a crucial parameter in deep learning techniques. But the medical image analysis datasets are very expensive to be built thus deep learning in small data regime i.e. training of time consuming and high sample complexity algorithms using limited resources is required. This kind of methodology has been proposed by Otalora et al., [16] in their work for exudate classification. They provided a label efficient CNN along with an active learning algorithm named as expected gradient length (EGL). The CNN model was based on LeNet network and it was trained using transfer learning approach A novel importance sampling approach to decrease false positive rate in the segmentation of exudates from retinal images has been presented by Sureshjani et al., [17] in their work for boosted exudates segmentation. This type of sampling during the training of network avoids the need of any post-processing steps. Their proposed methodology was based on a CNN with 9 ResNet blocks. These methods [15-17] are not multi-focal i.e. they are only focused towards segmentation of one kind of pathology at a time, while DR grading requires delineation of all retinal abnormalities simultaneously. Multi class CNNs had been employed classifying the presence/absence of multiple pathologies in retinal images. Tan *et al.,* [18] formulated a 10 layered neural network for detection of exudates, microaneurysms, and hemorrhages from retinal fundus images. They are not providing precise localization, i.e. pixel-wise segmentation of retinal pathologies.

In this paper, we have presented an end-to-end system utilizing an encoder-decoder based fully convolutional neural network that can perform pixelwise segmentation of multi-class retinal pathologies simultaneously for precise localization of their boundaries.

3 The Methodology

In this paper we propose to use an encoder-decoder based fully convolutional network architecture for semantic pixel-wise delineation of retinal pathology. The proposed network has adapted the well-known Segnet [19] where the network learns high dimensional intricate feature maps and provides pixel wise segmentation of retinal abnormalities by assigning particular object class label i.e. either 'exudates', 'hemorrhages', or 'cotton wool spots' to each pixel. **Fig. 2** depicts the main workflow of the proposed algorithm.

The input images are pre-processed before feeding them to the network. The following subsections illustrate the pre-processing techniques and network details.

3.1 Pre-processing

A pre-processing operation has been employed to obtain retinal images with normalized luminosity and enhanced contrast between retinal background and anatomical

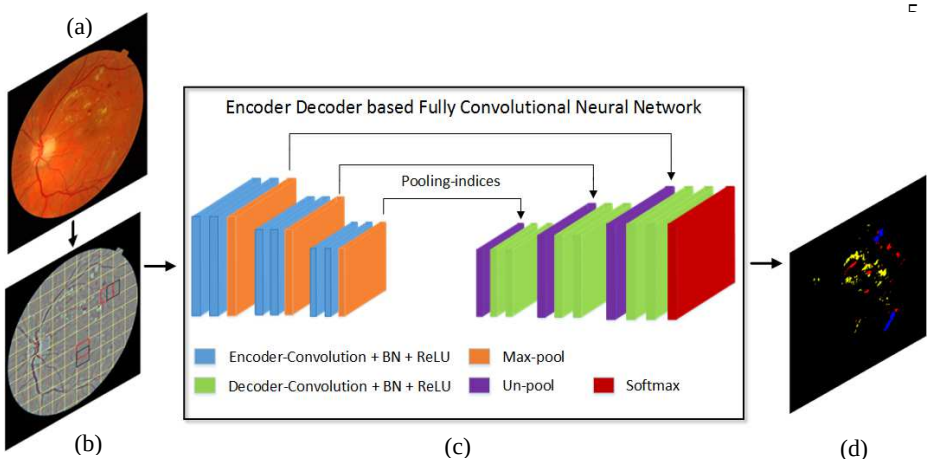

Fig. 2. (a) Input Retinal fundus image (b) Pre-processed image (c) Encoder Decoder based Fully Convolutional Neural Network (d) Segmented Pathology

structures. The principal of the pre-processing algorithm is a naïve linear transformation i.e. subtraction of estimated background image from original retinal image as presented in [20]. The estimate of background is computed by convolving the original image with a large arithmetic mean filter. The filter kernel size is not a pivotal parameter; it is adjusted so that the resultant background estimation doesn't contain any visible ocular structures. We have used a filter kernel of size 69×69. The normalized image (I_N) is obtained by pixel wise subtraction of the background estimated image (I_{BG}) from morphologically opened image (I_O) as represented in equation (1).

$$I_N(x,y) = I_O(x,y) - I_{BG}(x,y) \qquad (1)$$

The fluctuating brightness during the image acquisition process can introduce significant intensity variations among the images. Thus, it will become difficult to find a single best possible segmentation technique for all the images. Therefore, a global linear transformation function has been used for the purpose of shade correction, luminosity variation reduction, and contrast enhancement. The global transformation function will adjust the pixel values so that the complete range of gray levels (0 to 255, with reference to 8 bit images) is covered.

$$I_{ADJ}(x,y) = I_N(x,y) + 128 - I_{MAX\_PIXELS\_VAL}(x,y) \qquad (2)$$

$$I_H(x,y) = \begin{cases} 0, & I_N(x,y) < 0 \\ 255, & I_N(x,y) > 255 \\ I_{ADJ}(x,y), & \text{otherwise} \end{cases} \qquad (3)$$

The homogenized image (I_H) i.e. the shade corrected image is found by using equation (3) where I_N is the normalized image, and I_{ADJ} is the adjusted image. $I_{MAX\_PIXELS\_VAL}$ represents the pixel value with the maximum occurrence in the normalized imageI_N. The pixels with intensity values equal to $I_{MAX\_PIXELS\_VAL}$ belong to

the background of fundus image. The transformation will modify intensities of these pixels to 128; hence the other background pixels with different illumination conditions will standardize themselves around this value. This global transformation function is obtained by I_{ADJ} which is illustrated in equation (2). The retinal image obtained after illumination correction and contrast enhancement through the method mentioned in this section is shown in **Fig. 3**.

3.2 Patch-based Learning

The size of retinal lesions is small relative to the size of FOV, therefore, patch based learning has been employed which allows the deep network to precisely focus on the pathology. Moreover, the contextual information of pathology plays a pivotal role in decreasing the false positive rate. The relative location of pathology in retinal images is maintained by partitioning the images using overlapped windows. Overlapping patches are obtained via sliding a window with N x N dimensions over the retinal image with a stride of size 's'. The stride size is the proportion of overlap between adjacent grids e.g. N/2, N/4 etc. We have used stride size of N/2 for creating patches. Also, we propose to extract all the patches from the region which lies completely within the FOV because the region outside the FOV is of no practical importance.

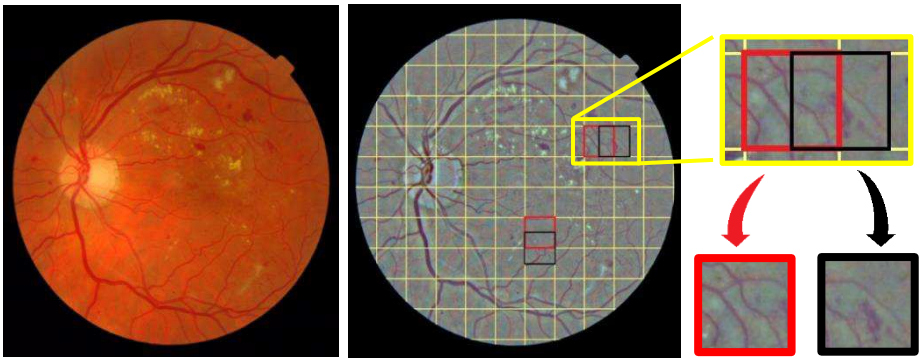

Fig. 3. (a) 3 Channel Retinal image (b) Pre-homogenized retinal image with 50% overlapping grids (c) Lesion at the edge of patch, may be misclassified (d) Complete lesion is contained in a single patch, less chance of misclassification

As depicted in **Fig. 3**, the overlapped grids prevent the patches with small pathology located at the edge to be misclassified as normal patches. This patch extraction method provides high quality candidates for the purpose of detecting retinal pathology.

3.3 Network Details

The basic building blocks of the network are convolution, up-sampling and sub sampling. The network has equal number of encoder and decoder blocks. These blocks are constructed using multiple convolutional, Batch Normalization (BN) [21] and

Rectified Linear Unit (ReLU) [22] layers. The only difference is sub sampling layer which is replaced with up-sampling layer in the case of decoders.
The proposed network has three encoder blocks and an equal number of decoder blocks proceeded by a pixel Classification layer. Each encoder block has two convolutional layers which extract a set of feature maps. The extracted feature maps are then batch normalized to reduce the sensitivity to network initialization. This is followed by the application of an element-wise threshold operation ReLU to each element of the input. Finally sub sampling (max pooling) operation is performed to obtain translation invariance and avoid overfitting, reduce memory consumption by providing an abstract representation of input to the network. The maximum feature value location (max-pooling indices) in each polling window is memorized for every feature map generated by an encoder; thus the segmentation resolution is improved.
Each encoder block has a corresponding decoder block, which unpools its input feature map using the max-pooling indices provided by the max-pooling layer of the encoder block. The up-sampled sparse feature maps are then fed into a convolutional layer which convolves them with trainable kernel banks to generate dense feature maps. These maps are then batch normalized and passed through non-linear ReLu layer. The second decoder block feeds the softmax layer [23] which classifies each pixel independently. The softmax classifier generates an M channel output image with each channel containing probability of every pixel belonging to a particular class, where M is the number of object classes. The size of the probability map generated by softmax layer is the same as that of the input image. The summary of the proposed encoder-decoder fully convolutional neural network is illustrated in **Table 1**.

3.4 Training Setup

The methodology has been evaluated on a dataset of 100 images with a train/test split of 90/10. The network is fed with image patches. The patch size is chosen in accordance with the smallest object present in input images to be segmented. We have chosen a patch size of 32x32 and stride size is maintained at '16'. The network is trained with 214021 image patches extracted from 90 pre-processed (homogenized) images for training. The weights of the network are initialized using the MSRA weight initialization method [24]. The dataset is biased because all images don't have equal number of pathological patches therefore class weighting method is used to make the network robust to majority class biasness. Overfitting is avoided by incorporating L_2 regularization [25] weight decay function with the value of regularization parameter 0.0005. The learning rate was initialized with the value 0.001 and was later updated during training in accordance with the loss value. Cross entropy loss function [26] with Stochastic Gradient Descent with Momentum (SGDM) optimization algorithm is used for adjusting the learning rate dynamically. A mini-batch size of 200 image patches is optimally selected along with shuffling of the image patches every epoch.

Table 1. Network Summary

	Layer Type	Filter kernel size	Stride	Padding	No. of feature maps
Input Encoder Block	Input	32×32×1	-	-	-
	Convolution	3×3×1	[1 1]	[1 1 1 1]	64
	BN	-	-	-	-
	ReLU	-	-	-	-
	Convolution	3×3×64	[1 1]	[1 1 1 1]	64
	BN	-	-	-	-
	ReLU	-	-	-	-
	Max Pooling	2×2	[2 2]	[0 0 0 0]	-
Output Decoder Block	Max Unpooling	-	-	-	-
	Convolution	3×3×64	[1 1]	[1 1 1 1]	64
	BN	-	-	-	-
	ReLU	-	-	-	-
	Convolution	3×3×64	[1 1]	[1 1 1 1]	4
	BN	-	-	-	-
	ReLU	-	-	-	-
	Softmax	-	-	-	-
	Pixel Classification Layer	-	-	-	-

4 Experimental Evaluation

4.1 Materials

The publically available dataset Messidor [27] is used for the experiments and evaluation purposes. The data-set is divided into 12 bases containing 1200 images in resolutions 2240x1488 and 1400x960. DR severity grade annotations are available publically for all the images but pathology based ground truths are not available. We have randomly selected 100 images from all the bases and retinal exudates, hemorrhages, and cotton wool spots are annotated by trained observers under the supervision of an ophthalmologist. The annotations are verified by trained ophthalmologist and clinicians from Armed Forces Institute of Ophthalmology (AFIO), Islamabad, Pakistan.

4.2 Performance Measures

The performance measures used to investigate the efficacy of the proposed algorithm are presented in **Table 2**.

Table 2. Performance Metrics for Retinal Image Analysis

Heading level	Description
Sensitivity (SN)	TP/TP+FN
Specificity (SP)	TN/TN+FP
Accuracy (Acc)	TP+TN/FOV pixel point

TP: True Positives TN: True Negatives
FP: False Positives FN: False Negatives

4.3 Quantitative Results

The attained SN, SP, and Acc are tabulated in **Table 3**. This table also provides a comparison of the quantitative measures of proposed algorithm against previously published algorithms. As presented in table, the proposed network has achieved highest accuracy in the segmentation task of exudates, hemorrhages, and cotton wool spots among other represented studies. Please note that the comparison is done against different datasets because image-based ground truth of these datasets is not available publically so proposed network can't be tested against them.

The pathology segmented by the proposed network and the ground truth overlaid on original retinal fundus images are depicted in **Fig. 4**.

Table 3. Comparison of Performance measures for pathology segmentation.

Algorithm	**Datasets**	**Exudates**			**Hemorrhages**			**Cotton wool spots**		
		Acc (%)	SP (%)	SN (%)	Acc (%)	SP (%)	SN (%)	Acc (%)	SP (%)	SN (%)
(Sinthanayothin *et al.*, 2002) [28]	Private database	-	99.7	88.5	-	88.7	77.5	-	-	-
(Fraz et al., 2017) [20]	Messidor	98.36	99.03	92.31	-	-	-	-	-	-
(Prentašic *et al.*, 2016) [15]	DRiDB	-	-	78	-	-	-	-	-	-
(Tan *et al*., 2017) [18]	CLEOP-ATRA	-	98.73	87.58	-	98.93	62.57	-	-	-
(Hashim *et al.*, 2014) [29]	Private database	-	-	-	-	-	-	74.53	76.49	71.78
(Bui *et al.*, 2017) [30]	DIARE-TDB1	-	-	-	-	-	-	85.54	84.4	85.9
Proposed Methodology	**Messidor**	**99.24**	**99.64**	**90.69**	**97.86**	**98.54**	**80.93**	**88.65**	**89.32**	**72.87**

5 Conclusion

In this research work we have presented an end to end fully convolutional encoder-decoder based network architecture for pixel wise simultaneous classification of retinal pathology into object classes: 'exudates', 'hemorrhages', 'cotton wool spots'. The techniques available in literature only focus on one or two of the pathological features. To the limit of our knowledge the proposed segmentation network is the first attempt of application of semantic segmentation networks for retinal pathology segmentation. The segmentation performance measures can be improved by using dilated convolutions i.e. atrous convolutions because they exponentially increase the field of view without decreasing the spatial dimensions.

This work has the ability to be incorporated in making an end to end computer aided diagnostic system for automatic and robust detection of retinal diseases. The developed approach helps in further optimization of pathology quantification module of the

QUARTZ software [31] which has been developed earlier by our research group. Moreover, we are planning to make the annotated dataset publically available, which enables other researchers to apply deep learning techniques for semantic segmentation of retinal pathologies.

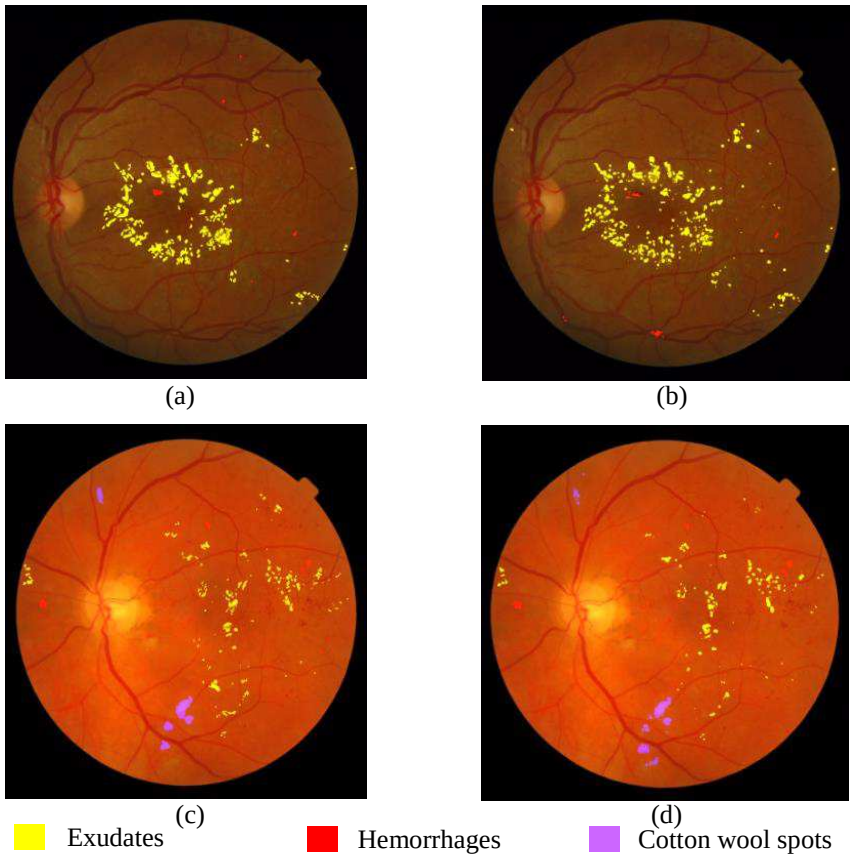

Fig. 4. Original retinal fundus (a, c) with overlaid ground truth (b, d) with overlaid predicted labels

References

1. Abràmoff, M.D., M.K. Garvin, and M. Sonka, *Retinal imaging and image analysis.* IEEE reviews in biomedical engineering, 2010. **3**: p. 169-208.
2. Organization, W.H., *Prevention of blindness from diabetes mellitus: report of a WHO consultation in Geneva, Switzerland, 9-11 November 2005*. 2006: World Health Organization.

3. Fraz, M.M. and S.A. Barman, *Computer Vision Algorithms Applied to Retinal Vessel Segmentation and Quantification of Vessel Caliber*, in *Image Analysis and Modeling in Ophthalmology* 2014, CRC Press. p. 49-84.
4. Fraz, M.M., et al., *Blood vessel segmentation methodologies in retinal images–a survey*. Computer methods and programs in biomedicine, 2012. **108**(1): p. 407-433.
5. Kanski, J.J. and B. Bowling, *Clinical ophthalmology: a systematic approach*. 2011: Elsevier Health Sciences.
6. Lahiri, A., et al. *Deep neural ensemble for retinal vessel segmentation in fundus images towards achieving label-free angiography*. in *Engineering in Medicine and Biology Society (EMBC), 2016 IEEE 38th Annual International Conference of the*. 2016. IEEE.
7. Fang, T., et al. *Retinal vessel landmark detection using deep learning and hessian matrix*. in *Image and Signal Processing (CISP), 2015 8th International Congress on*. 2015. IEEE.
8. Sopharak, A., et al., *Automatic detection of diabetic retinopathy exudates from non-dilated retinal images using mathematical morphology methods.* Computerized medical imaging and graphics, 2008. **32**(8): p. 720-727.
9. Walter, T., et al., *A contribution of image processing to the diagnosis of diabetic retinopathy-detection of exudates in color fundus images of the human retina.* IEEE transactions on medical imaging, 2002. **21**(10): p. 1236-1243.
10. Fraz, M.M., et al., *Ensemble Classification System Applied for Retinal Vessel Segmentation on Child Images Containing Various Vessel Profiles*, in *Image Analysis and Recognition*, A. Campilho and M. Kamel, Editors. 2012, Springer Berlin / Heidelberg. p. 380-389.
11. Lupascu, C.A., D. Tegolo, and E. Trucco, *FABC: Retinal Vessel Segmentation Using AdaBoost.* Information Technology in Biomedicine, IEEE Transactions on, 2010. **14**(5): p. 1267-1274.
12. Kanagasingam, Y., et al., *Progress on retinal image analysis for age related macular degeneration.* Progress in retinal and eye research, 2014. **38**: p. 20-42.
13. Sidibé, D., I. Sadek, and F. Mériaudeau, *Discrimination of retinal images containing bright lesions using sparse coded features and SVM.* Computers in biology and medicine, 2015. **62**: p. 175-184.
14. Sadek, I., D. Sidibé, and F. Meriaudeau. *Automatic discrimination of color retinal images using the bag of words approach*. in *SPIE Medical Imaging*. 2015. International Society for Optics and Photonics.
15. Prentašić, P. and S. Lončarić, *Detection of exudates in fundus photographs using deep neural networks and anatomical landmark detection fusion.* Computer Methods and Programs in Biomedicine, 2016. **137**: p. 281-292.
16. Otálora, S., et al., *Training Deep Convolutional Neural Networks with Active Learning for Exudate Classification in Eye Fundus Images*, in *Intravascular Imaging and Computer Assisted Stenting, and Large-Scale Annotation of Biomedical Data and Expert Label Synthesis*. 2017, Springer. p. 146-154.

17. Abbasi-Sureshjani, S., et al., *Boosted Exudate Segmentation in Retinal Images Using Residual Nets*, in *Fetal, Infant and Ophthalmic Medical Image Analysis*. 2017, Springer. p. 210-218.
18. Tan, J.H., et al., *Automated segmentation of exudates, haemorrhages, microaneurysms using single convolutional neural network.* Information Sciences, 2017. **420**: p. 66-76.
19. Badrinarayanan, V., A. Kendall, and R. Cipolla, *Segnet: A deep convolutional encoder-decoder architecture for image segmentation.* IEEE transactions on pattern analysis and machine intelligence, 2017. **39**(12): p. 2481-2495.
20. Fraz, M.M., et al., *Multiscale segmentation of exudates in retinal images using contextual cues and ensemble classification.* Biomedical Signal Processing and Control, 2017. **35**: p. 50-62.
21. Ioffe, S. and C. Szegedy, *Batch normalization: Accelerating deep network training by reducing internal covariate shift.* arXiv preprint arXiv:1502.03167, 2015.
22. Nair, V. and G.E. Hinton. *Rectified linear units improve restricted boltzmann machines*. in *Proceedings of the 27th international conference on machine learning (ICML-10)*. 2010.
23. Bishop, C., *Bishop cm: Pattern recognition and machine learning. springer.* Journal of Electronic Imaging, 2006. **16**(4): p. 140-155.
24. He, K., et al. *Delving deep into rectifiers: Surpassing human-level performance on imagenet classification*. in *Proceedings of the IEEE international conference on computer vision*. 2015.
25. Ng, A.Y. *Feature selection, L 1 vs. L 2 regularization, and rotational invariance*. in *Proceedings of the twenty-first international conference on Machine learning*. 2004. ACM.
26. Murphy, K.P., *Machine learning: a probabilistic perspective*. 2012.
27. Decencière, E., et al., *Feedback on a publicly distributed image database: the Messidor database.* Image Analysis & Stereology, 2014. **33**(3): p. 231-234.
28. Sinthanayothin, C., et al., *Automated detection of diabetic retinopathy on digital fundus images.* Diabetic medicine, 2002. **19**(2): p. 105-112.
29. Hashim, M.F. and S.Z.M. Hashim. *Diabetic retinopathy lesion detection using region-based approach*. in *Software Engineering Conference (MySEC), 2014 8th Malaysian*. 2014. IEEE.
30. Bui, T., N. Maneerat, and U. Watchareeruetai. *Detection of cotton wool for diabetic retinopathy analysis using neural network*. in *2017 IEEE 10th International Workshop on Computational Intelligence and Applications (IWCIA)*. 2017.
31. Fraz, M.M., et al., *QUARTZ: Quantitative Analysis of Retinal Vessel Topology and size – An automated system for quantification of retinal vessels morphology.* Expert Systems with Applications, 2015. **42**(20): p. 7221-7234.